

# Mass Transfer of Ni in Liquid Li Detected by Quartz Crystal Microbalance<sup>\*)</sup>

Leo IIZUKA and Masatoshi KONDO<sup>1)</sup>

*Tokyo Institute of Technology, School of Engineering,*

*Department of Mechanical Engineering, Graduate Major in Nuclear Engineering, Tokyo 152-8550, Japan*

<sup>1)</sup>*Tokyo Institute of Technology, Institute of Innovative Research, Laboratory for Advanced Nuclear Energy,  
Tokyo 152-8550, Japan*

(Received 10 November 2020 / Accepted 18 January 2021)

Liquid lithium (Li) is one of the tritium breeders of fusion reactors and the target material of advanced fusion neutron source. However, its chemical compatibility with structural materials is one of the important issues. Austenitic steels corrode due to the preferential depletion of Ni from their surface in liquid Li. However, the mass transfer behaviors of Ni in liquid Li at low temperature have been rarely studied. The purpose of the present study is to make clear the mass transfer behaviors of Ni in liquid Li by quartz crystal microbalance (QCM). The Ni electrode of the QCM unit got wet with liquid Li of approximately  $5.89 \times 10^{-2}$  cc at 473 K and 523 K for 600 seconds. The resonance frequency of the QCM unit changed due to the mass loss of the Ni electrode by the Ni dissolution into static liquid Li. The mass losses of Ni in liquid Li at 473 K and 523 K were obtained by Saurbrey's equation as  $6.60 \times 10^{-3}$  g/m<sup>2</sup> and  $1.27 \times 10^{-2}$  g/m<sup>2</sup>, respectively. The diffusion coefficient of Ni in static Li at 473 K was in the range between  $1.13 \times 10^{-10}$  and  $5.10 \times 10^{-10}$  m<sup>2</sup>/s by the model evaluation based on the Fick's second law. The diffusion coefficient at 523 K was in the range between  $1.90 \times 10^{-10}$  and  $6.87 \times 10^{-10}$  m<sup>2</sup>/s.

© 2021 The Japan Society of Plasma Science and Nuclear Fusion Research

Keywords: quartz crystal microbalance, liquid metal, mass transfer, corrosion, diffusion coefficient

DOI: 10.1585/pfr.16.2405026

## 1. Introduction

Liquid lithium (Li) is one of the tritium breeders of fusion reactors [1, 2]. The advanced fusion neutron source (A-FNS) is essential facility for the testing of structural materials under high-energy neutron irradiation. liquid Li target loop is one of the main components of the A-FNS facility [3, 4].

Austenitic steels are candidate structural materials of above-mentioned nuclear facilities [5–7], and the chemical compatibility with liquid Li is one of the important issues. The corrosion of austenitic steels in liquid Li was caused mainly by the preferential depletion of nickel (Ni) [7–11]. Liquid Li contaminates by the dissolution of Ni from austenitic steels during the operation of the facilities. Activation of Ni dissolved in liquid Li and its mass transfer in the nuclear facilities are also important issues. The metal impurities dissolved in liquid Li can be recovered with the cold trap, in which they are precipitates due to the low solubility at low temperature. The solubility and diffusivity of Ni in liquid Li are essential parameters to evaluate the mass transfer of Ni in the Li circulation loop, which equips the cold trap. However, these fundamental parameters at low temperature were rarely made clear so far.

Corresponding author's e-mail: [kondo.m.ai@m.titech.ac.jp](mailto:kondo.m.ai@m.titech.ac.jp)

<sup>\*)</sup> This article is based on the presentation at the 29th International Toki Conference on Plasma and Fusion Research (ITC29).

The dissolution of Ni in liquid Li at low temperature around 200°C is rather small, and the data of mass transfer is not easily obtained by means of immersion type corrosion tests. Quartz crystal microbalance (QCM) enables to precisely measure the mass change of the materials in fluids and gases around room temperature [12–14], though this technique has not been applied in liquid metal conditions.

The purpose of the present study is to make clear the mass transfer phenomena of Ni in liquid Li at low temperature by the QCM. The corrosion ratios of unalloyed Ni in liquid Li at 473 K and 523 K were evaluated by the QCM experiments. The diffusion coefficients of Ni in liquid Li were also obtained.

## 2. Experimental Conditions

### 2.1 Principle of quartz crystal microbalance (QCM)

The quartz crystal unit consists of the quartz crystal plate and the Ni electrodes, which are plated on the both sides of the plate. The quartz crystal plate oscillates due to the reverse piezoelectric effect, when AC voltage is applied to the QCM unit through the electrodes. Figure 1 shows the principle of the QCM to detect mass loss of Ni electrode by the dissolution in liquid Li. The wavelength of the

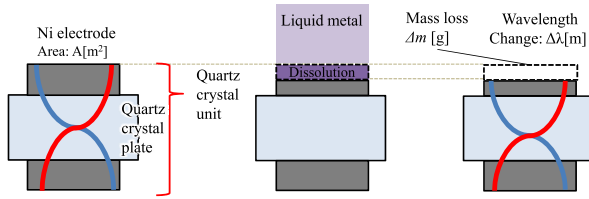


Fig. 1 Principle of QCM to detect mass loss of Ni electrode by its dissolution in liquid Li.

quartz crystal unit becomes shorter when the Ni electrode becomes thinner due to the dissolution in liquid Li. The change of wave length corresponds to that of resonance frequency expressed as;

$$\Delta f = \frac{v}{\lambda + \Delta\lambda} - \frac{v}{\lambda} = -\frac{v\Delta\lambda}{\lambda^2 + \lambda\Delta\lambda} \sim -\frac{v}{\lambda^2} \Delta\lambda, \quad (1)$$

where  $\Delta f$ ,  $\lambda$ ,  $\Delta\lambda$  and  $v$  are the change of frequency [Hz], the wave length [m], the change of wave length [m], and the wave velocity [m/s], respectively. The frequency change was measured by the QCM analyzer. The mass loss of the metal electrode is then obtained from the change of frequency by Saurbrey's equation [12];

$$\Delta f = -\frac{2f_0^2}{A\sqrt{C_{shear} \times \rho}} \Delta m, \quad (2)$$

where  $\Delta f$ ,  $f_0$ ,  $A$ ,  $C_{shear}$ ,  $\rho$ , and  $\Delta m$  are the change of frequency [Hz], the resonance frequency of the quartz crystal [Hz], the electrode area [ $\text{cm}^2$ ], the shear stiffness [ $\text{g}/\text{cm}/\text{s}^2$ ], the density of crystal [ $\text{g}/\text{cm}^3$ ], and the mass change [g], respectively.

### 2.2 Experimental conditions

Figure 2 shows the apparatus of mass transfer tests with liquid Li. The quartz crystal unit is AT-cut quartz crystal plate which has Ni electrodes plated on the both sides. The size of the plate was 8.5 mm square. The diameter of Ni working electrode was 5 mm, and its thickness was 100 nm. The resonance frequency and resistance of the quartz crystal unit were measured in air atmosphere at room temperature before the mass transfer test with liquid Li. The measurement of the resonance frequency and resistance was conducted with the QCM analyzer (Seiko EG & G, model QCM922A), which can measure resonance frequency from 5 to 30 MHz with  $1 \times 10^{-2}$  seconds and the resolution of 0.01 Hz.

The mass transfer tests were performed in the globe box filled with argon (Ar) having the purity of 99.99%. The quartz crystal unit was installed on the glass plate, which was placed on the plate heater. Solid Li of approximately  $5.89 \times 10^{-2}$  cc was installed on the Ni electrode using the cylinder made of 316 austenitic steel (Fe-18Cr-12Ni-2Mo), which had an inner diameter of 5 mm. Table 1 presents metal and non-metal impurities of liquid Li. The test temperature was 473 K and 523 K, and much lower than the phase transition temperature of quartz crystal at

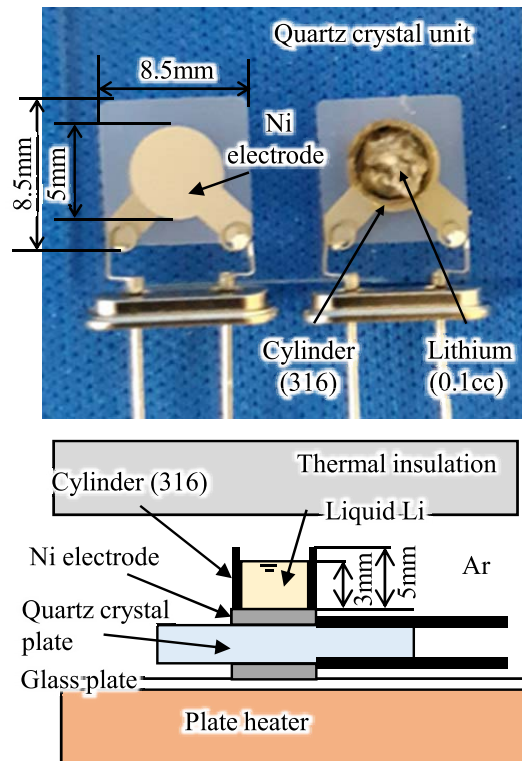
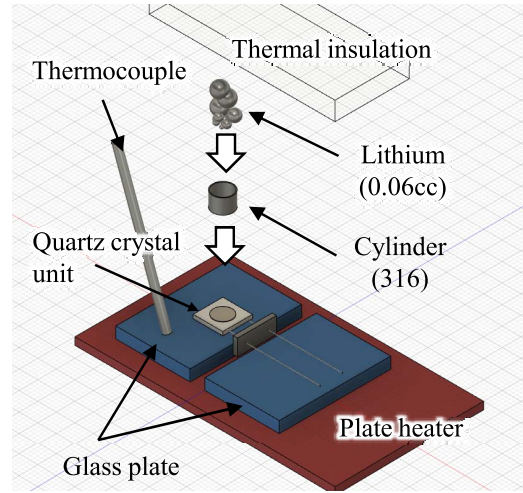


Fig. 2 Experimental apparatus of liquid Li mass transfer test.

approximately 773 K [15]. The test duration was 600 seconds.

The Rayleigh number of liquid Li installed in the cylinder was estimated in equation of;

$$Ra = \frac{g\beta}{\nu\alpha} L^3 \Delta T, \quad (3)$$

where  $g$ ,  $\alpha$ ,  $\beta$ ,  $\nu$ ,  $\Delta T$ , and  $L$  are the gravitational acceleration [ $\text{m}/\text{s}^2$ ], the thermal diffusivity of liquid Li [ $\text{m}^2/\text{s}$ ], the coefficient of thermal expansion of liquid Li [ $1/\text{K}$ ], the kinetic viscosity of liquid Li [ $\text{m}^2/\text{s}$ ], the temperature gradient in liquid Li [K], and the thickness of liquid Li [m], respectively. The inventory of liquid Li was quite small as approximately  $5.89 \times 10^{-8} \text{ m}^3$  and the apparatus was thermally insulated. When the temperature gradient in liquid

Table 1 Metal and non-metal impurities of Li (unit: wppm).

	Na	Ca	K	Fe	Si	N	Cl
Li	40	10	10	10	10	70	10

Table 2 Results of QCM tests in Ar and liquid Li at 473K and 523K for 600 seconds.

	Temperature [K]	Duration [s]	Change of Resonance resistance [ $\Omega$ ]	Change of Resonance frequency [Hz]	Mass loss of Ni [g]	Mass loss of Ni per unit area [ $\text{g}/\text{m}^2$ ]
Ar	473	600	-2.84	3.12	$3.29 \times 10^{-9}$	$1.68 \times 10^{-4}$
	523		3.05	9.88	$1.04 \times 10^{-8}$	$5.31 \times 10^{-4}$
Li	473	600	-1.42	$1.23 \times 10^2$	$1.30 \times 10^{-7}$	$6.61 \times 10^{-3}$
			-3.43	$2.21 \times 10^2$	$2.33 \times 10^{-7}$	$1.19 \times 10^{-2}$
			-1.11	$2.44 \times 10$	$2.58 \times 10^{-8}$	$1.31 \times 10^{-3}$
		Average		$1.23 \times 10^2$	$1.30 \times 10^{-7}$	$6.60 \times 10^{-3}$
Li	523	600	6.04	$3.67 \times 10^2$	$3.88 \times 10^{-7}$	$1.97 \times 10^{-2}$
			-5.62	$2.09 \times 10^2$	$2.20 \times 10^{-7}$	$1.12 \times 10^{-2}$
			-3.74	$1.35 \times 10^2$	$1.43 \times 10^{-7}$	$7.27 \times 10^{-3}$
		Average		$2.37 \times 10^2$	$2.50 \times 10^{-7}$	$1.27 \times 10^{-2}$

Li was assumed to be 5 K, the Raleigh number at 473 K and 523 K were approximately 5.2. This value was much less than the critical Ra number of 1700. Thus, the Li mass transfer tests were performed at a static condition, in which the mass transfer was not promoted by the thermal convection.

After the Li mass transfer test, the quartz crystal unit was taken out from the globe box. The quartz crystal unit was cleaned with water and ethanol to remove Li from the electrode surface. The resonance frequency and resistance of the quartz crystal unit were then measured in air atmosphere at room temperature.

The effect of heat treatment on the performance of the quartz crystal unit was also investigated in the same manner with the liquid Li mass transfer test. The quartz crystal units were heated under Ar atmosphere without the installation of liquid Li. The temperature conditions were 473 K and 523 K. The test duration was 600 seconds. The quartz crystal unit was cleaned with water and ethanol after the heating. The resonance frequency and resistance of the quartz crystal unit were measured in air atmosphere.

The resonance resistance of the quartz crystal unit changes when the quartz crystal plate is damaged in the mass transfer test. In this case, the frequency change due to the mass loss of the Ni electrode is affected by the damage. Therefore, small change of the resonance resistance was also checked after the liquid Li test.

### 3. Experimental Results

Table 2 presents the summary of experimental re-

sults. The resonance frequency of the quartz crystal unit before and after the heat treatment without Li installation under Ar atmosphere at 473 K were 9063935 Hz and 9063938 Hz, respectively. The change of the resonance frequency was negligibly small. In the same way, the change of the resonance frequency was negligibly small in the test at 523 K. These results indicated that the performance of the quartz crystal unit was not affected by the heat treatment at the test temperatures under Ar atmosphere.

The change of the resonance frequency by the mass transfer tests in liquid Li at 473 K was  $1.23 \times 10^2$  Hz in average. The change of the resonance resistance in the test was negligibly small as the same as that in the heat treatment test under Ar atmosphere. The frequency change became larger when the test temperature was higher, since the mass loss of Ni electrode in liquid Li due to its dissolution became larger at higher temperature. Figure 3 shows the mass loss of Ni in liquid Li. The mass loss of Ni in the test at 473K corresponds to  $1.31 \times 10^{-7}$  g according to Eq. (2). This mass loss is too small to be detected by electro reading balances. In the same way, the change of the resonance frequency by the tests in liquid Li at 523 K was  $2.37 \times 10^2$  Hz in average. the mass loss of Ni in liquid Li at 523 K was  $2.50 \times 10^{-7}$  g.

The dispersion of the experimental data was possibly due to the loss of Ni in the cleaning procedure of the quartz crystal unit. The adhesion of Li oxides and/or Li hydro oxides on the electrode surface is also the possible cause of the dispersion. The increase of Ni concentration in liquid

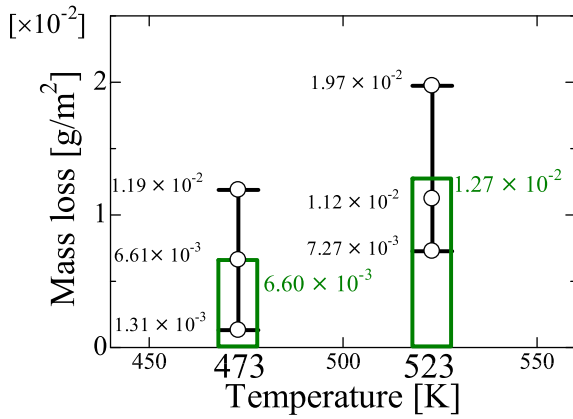


Fig. 3 Mass losses of Ni electrode in liquid Li at 473 K and 523 K for 600 seconds.

Li in the mass transfer tests was in the range between  $8.54 \times 10^{-5}$  and  $1.28 \times 10^{-3}$  wt%.

#### 4. Discussions

The dissolution and diffusion of Ni from the Ni electrode into liquid Li at static condition were discussed here. The Ni concentration in liquid Li on the phase interface was assumed to be equal to the saturate condition. The solubility of Ni in liquid Li was larger than the other elements such as Fe and Cr [10, 16, 17]. The data of the Ni solubility in liquid Li was measured in the temperature range between 773 K - 1000 K and reported in the literatures [10, 16, 17] as summarized in Fig. 4. The Ni solubility at the temperature range between 473 K - 600 K was not available in the previous studies. The temperature dependence of the solubility proposed by Beskorovaniyi [16] was close with that by Leavenworth [17]. The solubility proposed by Lyublinski [10] had larger temperature dependence than the other solubility data. The temperature conditions of the solubility data by Lyublinski were close to our experimental conditions. The solubilities by Beskorovaniyi and Leavenworth are one order larger than that by Lyublinski at the temperature of the current work, when these solubility data were linearly extrapolated to the temperature conditions of the current work. The solubility data with small contribution of unique data by ref. [10] can be obtained by the arithmetic mean. The solubility data with the influence of unique data [10] can be obtained by the geometric mean. The Ni solubilities in liquid Li at the low temperature are then obtained by both the arithmetic mean and the geometric mean of the values extrapolated from the equations of the three literatures [10, 16, 17]. The Ni solubility by the arithmetic mean of the literature data ( $C_{s,arithmetic}$ , [at%]) and that by the geometric mean ( $C_{s,geometric}$ , [at%]) at 473 K are obtained as  $5.24 \times 10^{-4}$  and  $2.49 \times 10^{-4}$  at%, respectively.  $C_{s,arithmetic}$  and  $C_{s,geometric}$  at 523 K are obtained as  $7.80 \times 10^{-4}$  and  $4.15 \times 10^{-4}$  at%, respectively. They are formulated as follows;

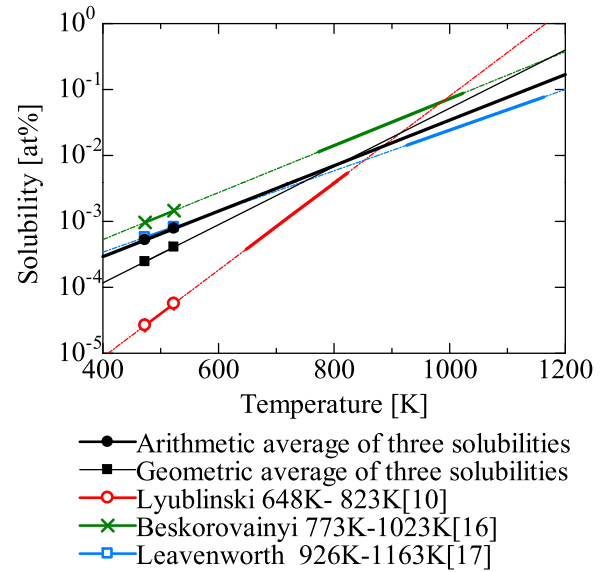


Fig. 4 Ni solubilities in liquid Li [10, 16, 17].

$$C_{s,arithmetic}[\text{at}\%] = 1.22 \times 10^{-5} \exp(7.95 \times 10^{-3}T), \quad (4)$$

$$C_{s,geometric}[\text{at}\%] = 2.00 \times 10^{-6} \exp(1.02 \times 10^{-2}T), \quad (5)$$

where  $T$  is the liquid Li temperature [K].

The chemical diffusion of Ni impurity in liquid Li was evaluated based on the Fick's second law as;

$$\frac{\partial C_{(x,t)}}{\partial t} = D \frac{\partial^2 C_{(x,t)}}{\partial x^2}, \quad (6)$$

where  $C_{(x,t)}$ ,  $D$ ,  $t$  and  $x$  are the Ni concentration [at%] at the time of  $t$  [s] and at the location of  $x$  [m], the diffusion coefficient of Ni in liquid Li [ $\text{m}^2/\text{s}$ ], the time [s] and the distance [m], respectively. Equation (6) is approximated as;

$$\frac{C_{(x,t)} - C_0}{C_s - C_0} = 1 - \operatorname{erf} \frac{x}{2\sqrt{Dt}}, \quad (7)$$

where  $C_0$  is the initial concentration of Ni [at%] in liquid Li. The mass losses of the Ni electrode in liquid Li at 473 K and 523 K for 600 seconds were obtained from Eq. (2). The mass loss corresponds to the dissolution of Ni into liquid Li, and is given by the integration of Ni concentration in a thickness direction of liquid Li as;

$$\begin{aligned} \frac{\Delta m}{S} &= \frac{M_{\text{Ni}} * \rho_{\text{Li}}}{M_{\text{Li}}} \int_0^L C \, dx \\ &= \frac{M_{\text{Ni}} * \rho_{\text{Li}}}{M_{\text{Li}}} \int_0^L C_s \left(1 - \operatorname{erf} \frac{x}{2\sqrt{Dt}}\right) dx, \end{aligned} \quad (8)$$

where  $\Delta m$ ,  $S$ ,  $M_{\text{Ni}}$ ,  $M_{\text{Li}}$ ,  $\rho_{\text{Li}}$ , and  $L$  are the dissolution of Ni [g], the Li contact area [ $\text{m}^2$ ], the atomic weight of Li, the atomic weight of Ni, the density of liquid Li [ $\text{g}/\text{m}^3$ ], and the thickness of liquid Li [m], respectively. Here,  $L$  was 3 mm and  $t$  was 600 seconds. The diffusion coefficients

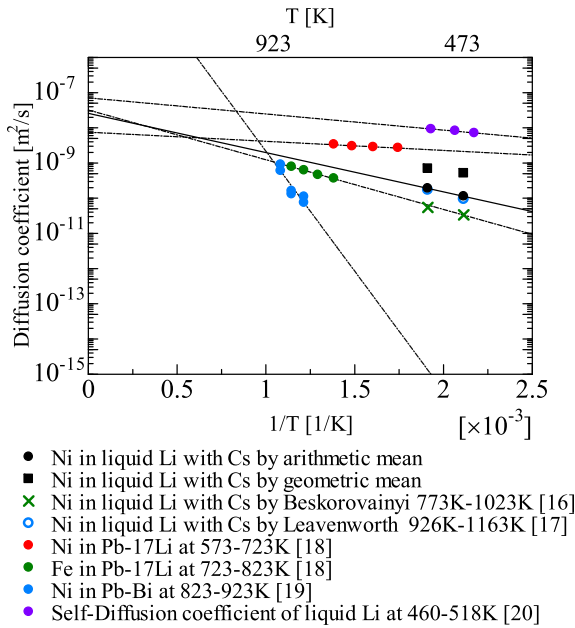


Fig. 5 Diffusion coefficients of Ni and Fe in liquid metals (Li, Pb-17Li and Pb-Bi) in current and previous experimental studies.

of Ni in liquid Li at 473 K and 523 K with  $C_{s,arithmetic}$  and  $C_{s,geometric}$  were obtained from Eqs. (4), (5), and (8). The diffusion coefficients obtained from Eq. (8) with  $C_{s,arithmetic}$  ( $D_a$ , [m<sup>2</sup>/s]) at 473 K and 523 K are obtained as  $1.13 \times 10^{-10}$  and  $1.90 \times 10^{-10}$  m<sup>2</sup>/s, respectively. Those with  $C_{s,geometric}$  ( $D_g$ , [m<sup>2</sup>/s]) at 473 K and 523 K are obtained as  $5.10 \times 10^{-10}$  and  $6.87 \times 10^{-10}$  m<sup>2</sup>/s, respectively. They are formulated as;

$$D_a[\text{m}^2/\text{s}] = 2.59 \times 10^{-8} \exp(-2.13 \times 10^4/RT), \quad (9)$$

$$D_g[\text{m}^2/\text{s}] = 1.15 \times 10^{-8} \exp(-1.22 \times 10^4/RT), \quad (10)$$

where R is the gas constant (8.314 J/molK). Figure 5 shows the diffusion coefficients of Ni in liquid Li and the comparison with the other diffusion coefficients in some liquid metals. The graph legends of solid circle, solid square, cross, and open square in Fig. 5 indicate the diffusion coefficients obtained with the Ni solubilities which were indicated by the same legends in Fig. 4. The temperature dependence of the Ni diffusivity in liquid Li was close to that in liquid Pb-17Li [18] and smaller than that in liquid Pb-Bi [19].

Figure 6 shows the mass loss of the Ni electrode compared with that of steels (304 austenitic steel (Fe-17Cr-10Ni-2Mo) and F82H (Fe-8Cr-2W)) in liquid Li at static conditions [6, 21]. The mass loss data of Ni in the current work agreed well with the time dependence of mass loss of 304 steel, which contained Ni as the major alloying element. This trend indicated that the Ni dissolution was dominant factor for the corrosion of austenitic steel in liquid Li due to the large solubility of Ni in liquid Li. The effect of exposure time on the corrosion mass loss of F82H

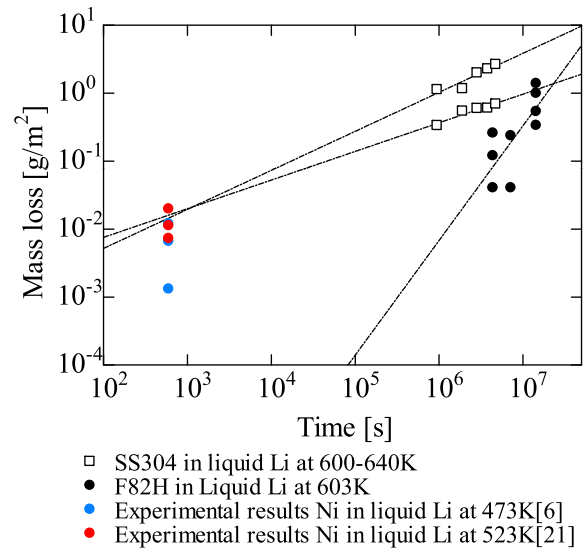


Fig. 6 Time dependence of mass loss of Ni in liquid Li in current and previous experimental studies.

in liquid Li is large rather than that of Ni bearing materials, since the corrosion is caused by the chemical interaction involving some non-metal impurities (i.e., nitrogen and oxygen), and it is promoted by the exposure for longer time.

## 5. Conclusion

Major conclusions are follows;

1. The mass transfer phenomena of Ni in liquid Li in the temperature range between 473 K and 523 K were studied by means of the QCM experiments. The mass loss of Ni in liquid Li at 473 K was  $6.60 \times 10^{-3}$  g/m<sup>2</sup> and that at 523 K was  $1.27 \times 10^{-2}$  g/m<sup>2</sup>.
2. The diffusion coefficients of Ni in liquid Li were obtained from the experimental results. Previous literatures indicate that the Ni solubility in liquid Li at 473 K is in the range between  $2.49 \times 10^{-4}$  at% and 5.24 at%. The Ni solubility at 523 K is in the range between  $4.15 \times 10^{-4}$  at% and  $7.80 \times 10^{-4}$  at%. The theoretical model based on the Fick's second law indicates that the diffusion coefficient of Ni in liquid Li at 473 K is in the range between  $1.13 \times 10^{-10}$  m<sup>2</sup>/s and  $5.10 \times 10^{-10}$  m<sup>2</sup>/s. The coefficient at 523 K is in the range between  $1.90 \times 10^{-10}$  and  $6.87 \times 10^{-10}$  m<sup>2</sup>/s.

## Acknowledgement

The authors acknowledge Mr. T. Koga of Toyo Corporation and Mr. Y. Yamamoto of Seiko EG and G for their technical assistance and fruitful discussions on the QCM experiment. Mrs. Y. Tamai and Mr. M. Imai of Tokyo Institute of Technology for their technical assistance in QCM experiments.

- [1] T. Muroga, M. Gasparotto and S.J. Zinkle, *Fusion Eng. Des.* **61-62**, 13 (2002).
- [2] M. Kondo, T. Tanaka, S. Fukada and T. Valentyn, *Comprehensive Nuclear Materials 2nd edition* **6**, 176 (2020).
- [3] S. Sato, M. Nakamura, S. Kwon, M. Ohta, C. Park, M. Oyaidzu, K. Ochiai, A. Kasugai, K. Sakamoto and S. Ishida, *Fusion Eng. Des.* **155**, 111714 (2020).
- [4] A. Kasugai, K. Kasuya, H. Kobayashi, H. Kondo, S. Kwon, M. Nakamura, K. Ochiai, M. Ohta, M. Oyaidzu, C. Park, S. Sato and M. Teduka, *PASJ2018, Nagaoka, Japan, THOL08*, 110 (2018).
- [5] M. Kondo, V. Tsisar, T. Muroga, T. Nagasaka and O. Yeliseyeva, *Plasma Fusion Res.* **9**, 294 (2010).
- [6] X. Meng, G. Zuo, W. Xu, Z. Sun, M. Huang, X. Yuan, C. Xu, W. Hu, D. Andruczyk, J. Hu and H. Deng, *Fusion Eng. Des.* **128**, 75 (2018).
- [7] J. Qian, J. Chen, J. Chen, Z. Xu, W. Wang and C. Pan, *J. Nucl. Mater.* **179-181**, 603 (1991).
- [8] T. Suzuki, *ISIJ* **75-11**, 35 (1989).
- [9] Q. Xu, M. Kondo, T. Nagasaka, T. Muroga, M. Nagura and A. Suzuki, *Fusion Eng. Des.* **83**, 1477 (2008).
- [10] I.E. Lyublinski, V.A. Evtikhin, V.Yu. Pankratov and V.P. Krasin, *J. Nucl. Mater.* **224**, 288 (1995).
- [11] F. Tortorelli, *J. Nucl. Mater.* **191-194**, 965 (1992).
- [12] G. Saubrey, *Zeitschrift für Physik* **155**, 206 (1959).
- [13] K. Kanazawa and J. Gordon, *Anal. Chim. Acta* **175**, 99 (1985).
- [14] K.J. Choia, Y.H. Kima, S.M. Changa, A. Egawab and H. Muramatsu, *Anal. Chim. Acta* **386**, 229 (1999).
- [15] K.S.P. Karunadasa, C.H. Manaratne, H.M.T.G.A. Pitawala and R.M.G. Rajapakse, *J. Phys. Chem. Solids* **117**, 131 (2018).
- [16] N.M. Beskorovainyi, A.G. Itoltukhovskii, I.E. Lyublinskii and V.K. Vasil'ev, *UDC 621. 039. 53* (1981).
- [17] H.W. Leavenworth and R.E. Cleary, *Acta Metall.* **9**, 519 (1961).
- [18] Y. Gao, M. Takahashi and M. Nomura, *Energy Procedia* **71**, 313 (2015).
- [19] Y. Gao, M. Takahashi, M. Nomura and T. Nozawa, *Fusion Eng. Des.* **109-111**, 1604 (2016).
- [20] J.S. Murday and R.M. Cotts, *J. Chem. Phys.* **48**, 4938 (1968).
- [21] P. Favuzza, A. Aiello, A. Antonelli, M. Cuzzani, G. Fasano, M. Granieri, S. Mannori, G. Micciche, F.S. Nitti, M. Tarantino and A. Tincani, *Fusion Eng. Des.* **136**, 1417 (2018).